Journal of Materials Chemistry A

PAPER

View Article Online
View Journal

Cite this: DOI: 10.1039/c6ta10538f

Hydrogen weakens interlayer bonding in layered transition metal sulfide $Fe_{1+x}S$†

Aravind Krishnamoorthy,[ab] Minh A. Dinh[ac] and Bilge Yildiz*[abc]

The presence of interlaminar interstitial defects like hydrogen affects the mechanical properties of van der Waals-bonded layered materials such as transition metal chalcogenides. While the embrittling effect of hydrogen is well understood in metals, the impact of hydrogen defects on the mechanical behavior of layered chalcogenides remained unexplored. In this article, we use density functional calculations to reveal the influence of different hydrogen point defects on important mechanical metrics, including binding energies, elastic moduli and tensile and shear strengths of a prototypical ionic layered material, mackinawite, $Fe_{1+x}S$. We find that one of the low-energy hydrogen defect structures, interlaminar molecular H_2 interstitials, severely degrades the strength of inter-layer van der Waals interactions in the mackinawite crystal. This leads to a significant (over 80%) degradation in the mechanical properties of the mackinawite crystal and enables facile interlayer sliding and exfoliation. This finding suggests the mechanisms for cathodic exfoliation of transition metal chalcogenides like $Fe_{1+x}S$, and presents a plausible mechanism for the poor protectiveness of layered passive films like mackinawite that undergo failure by spalling or delamination.

Received 7th December 2016
Accepted 7th February 2017

DOI: 10.1039/c6ta10538f

rsc.li/materials-a

1. Introduction and motivation

The behavior of hydrogen point defects in layered, van der Waals-bonded crystals is of central importance to several applications like electrochemical hydrogen generation,[1] hydrogen storage,[2] and two-dimensional crystal synthesis by exfoliation.[3] In most of these studies, the problem of interest is the effect of such point defects on the mechanical properties of the host crystal. A specific example is found in the industrially important case of 'sour' corrosion of steels, where surface passive films containing layered iron sulfides like mackinawite act as the primary barrier layer protecting the underlying steel surface against further corrosion and hydrogen embrittlement.[4,5] This nominally passive layer helps measurably to reduce the overall corrosion rate and remains protective as long as it retains its physical integrity.[6] Under continued corrosion, this passive film undergoes spallation leading to exposure of the bare metal and subsequent catastrophic localized corrosion.[5,6] Therefore, understanding the mechanisms behind mechanical failure of these layered systems in electrochemical environments is critical to improve the service lifetime of steels under sour corrosive conditions.

There are several studies, both experimental and computational, that explain the embrittling role of hydrogen in compromising the mechanical properties on compact (*i.e.* not van der Waals bonded) crystals like metals,[7] semiconductors[8] and oxides.[9,10] While there are investigations into the impact of intercalating ions and molecules on the mechanical properties of layered systems,[11–13] primarily in the context of electrochemical exfoliation of two-dimensional crystals, a similarly rigorous analysis of the role of different hydrogen defects is lacking.

To address this problem, we use density functional theory calculations (details in Section 2) to identify dominant hydrogen defects in mackinawite based on their formation energies and quantify their effect on the mechanical properties of mackinawite by mapping stress–strain behavior. Section 3 describes how molecular H_2 interstitials in low concentrations can significantly degrade the inter-layer van der Waals bonding and enable easy interlayer sliding and exfoliation of mackinawite crystals and explains this behavior in analogy to interstitials and intercalants in other layered systems. The implications of this loss of mechanical stability for protectiveness of mackinawite films and for exfoliation strategies for other layered compounds are discussed in Section 4.

2. Methodology and computational details

The first step in understanding the impact of hydrogen defects on the mechanical properties of mackinawite is to identify

[a]Laboratory for Electrochemical Interfaces, Massachusetts Institute of Technology, 77 Massachusetts Avenue, Cambridge, MA 02139, USA. E-mail: byildiz@mit.edu
[b]Department of Materials Science and Engineering, Massachusetts Institute of Technology, 77 Massachusetts Avenue, Cambridge, MA 02139, USA
[c]Department of Nuclear Science and Engineering, Massachusetts Institute of Technology, 77 Massachusetts Avenue, Cambridge, MA 02139, USA

† Electronic supplementary information (ESI) available. See DOI: 10.1039/c6ta10538f

thermodynamically stable hydrogen defects. We calculate formation energies of different hydrogen defect configurations to identify the most stable defect structures expected to exist at moderate temperatures around 200 °C encountered under sour corrosion conditions.

We then compare the mechanical properties of hydrogen-containing mackinawite crystals to those of hydrogen-free mackinawite crystals by computing virtual stress–strain diagrams for two modes of displacement chosen to reflect the strength of the interlayer bond, namely strains along the z-direction, ε_{zz} (simulating a uniaxial tensile test along the z-direction) and shear strain along a plane perpendicular to the z-direction, γ_{xz} and γ_{yz}. These virtual stress–strain diagrams give us two important metrics, namely the elastic modulus and the stress to failure, which are then compared among calculations of different hydrogen defect structures.

All Density Functional Theory (DFT) calculations[14] were carried out with the projector augmented wave method[15] using the Perdew–Burke–Ernzerhof (PBE) form of Generalized Gradient Approximation (GGA) functional[16] implemented in the Vienna Ab initio Simulation Package (VASP).[17,18] For accurate reproduction of the mackinawite electronic structure, the DFT+U method was used with the previously determined value of $U - J = 1.6$ eV that was found to be suitable for iron chalcogenide phases.[19] Plane wave components up to 350 eV were included to avoid wrap-around errors and integrations in the reciprocal space were performed on a $6 \times 6 \times 6$ Monkhorst–Pack grid that includes 27 non-equivalent points in the Brillouin zone.[20] For defect formation energy calculations, computations were performed on a $2\sqrt{2} \times 2\sqrt{2} \times 2$ unit cell containing 32 formula units and total energies were converged to within 10^{-5} eV in each self-consistency cycle. The forces on ions were converged to within 0.01 eV Å^{-1}.

Stress–strain curves are plotted by calculating the internal stresses in the crystal as strains are increased in uniform increments of 0.04. For these high-accuracy calculations, atoms in the crystal were relaxed until forces on each atom are less than 10^{-3} eV Å^{-1} and all other stress components are less than 5 MPa. In keeping with previous studies, we use the internal stress tensor computed directly by VASP because it avoids the numerical errors associated with the manual calculation of the derivative of the system energy. Previous calculations have shown these two approaches to be identical in the case of another layered system, graphite.[21]

There are conflicting reports on the ground state magnetic configuration of mackinawite, with previous studies that support both antiferromagnetic[22] and non-magnetic[23] configurations. In this work, the non-magnetic configuration was found to have a lower system energy, consistent with previous simulations as well as experiments.[24] Therefore, in this work, we use the non-magnetic form of the crystal for all calculations. We further confirm that hydrogen point defect formation energies calculated in this work are within 0.05 eV of the formation energy calculated from a spin-unrestricted simulation of the antiferromagnetic crystal.

Accurately modeling van der Waals forces are essential for modeling the mechanical properties of layered systems. Since semilocal functionals like PBE do not include long-range electronic correlation effects, we use Grimme's DFT-D2 formulation of dispersion interactions to explicitly account for them.[25] While semi-empirical in nature, this approach has previously demonstrated good accuracy in calculating elastic constants in graphite and MoS_2.[26] Where possible, we have also calculated stress–strain behavior using the optB86b-vdW functional, one of a class of parameter-free formulations of van der Waals-functionals.[27] Since the results from the optB86b-vdW functional are qualitatively similar to that of the DFT-D2 method (see ESI†), we will restrict our discussion in Section 3 to DFT-D2 results.

3. Results and discussion

Previous studies have established that the mechanical response of the hydrogen-doped crystal depends strongly on the specific nature of the hydrogen defect. Section 3.1 describes the identification of sulfur-bonded monoatomic hydrogen interstitial and the interlayer H_2 interstitial as the most stable hydrogen defects in mackinawite. Consequently, only these two defects are analyzed for their impact on mackinawite's mechanical properties. Sections 3.2 and 3.3 show how one of these defect structures, the H_2 interstitial, is responsible for a 90% decrease in the van der Waals bonding strength between mackinawite sheets. The implication of this observation for the performance of mackinawite as a passive film and prospects for intentional functionalization of this phenomenon are discussed in Section 3.4.

3.1. H defect chemistry in mackinawite

We calculate defect formation energies for two classes of hydrogen point defects, H atoms substituting the Fe^{2+} or S^{2-} lattice sites and interstitial H atoms at three crystallographically non-equivalent sites as shown in Fig. 1. We limit our calculations to neutral H defects in all cases because the metallic mackinawite films[28] do not admit the presence of charged point defects unlike semiconducting oxides.[10] In addition to these point defects, layered compounds also admit another type of point defect, namely the molecular hydrogen interstitial in the interlayer space. In particular, the H_2 molecule in mackinawite occupies the large tetrahedral void formed between the S^{2-} ions from adjacent layers (Fig. 1f).

Defect formation energies are calculated using the formula

$$\Delta G_f^i = E(\mathrm{FeS}\cdot\mathrm{H_i}) - E(\mathrm{FeS}) + eU + 2.3k_B T\mathrm{pH}$$

where ΔG_f^i is the free energy of formation of the hydrogen defect, $E(\mathrm{FeS}\cdot\mathrm{H_i})$ and $E(\mathrm{FeS})$ are DFT-calculated energies of the hydrogen-containing and hydrogen-free mackinawite crystal, e is the magnitude of electronic charge, U is the electrostatic potential of the mackinawite crystal relative to the standard hydrogen electrode, T is the temperature and k_B and pH have their usual meanings. For all formation energies, we use $U = -0.5$ V relative to the Standard hydrogen electrode (SHE), pH = 5, and $T = 200$ °C to reflect conditions that are encountered in sour corrosion. The formation energies for substitutional

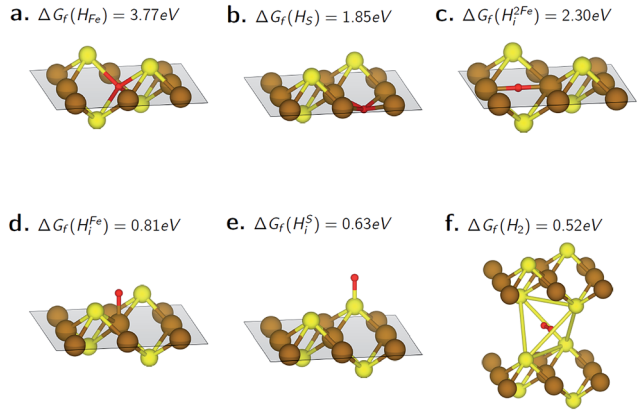

Fig. 1 Hydrogen point defect structures considered in this study along with formation energies. Brown, yellow and red spheres represent iron, sulfur and hydrogen atoms, respectively. Dashed lines are guides for the eye that shows the S–Fe–S basal layer. (a and b) are substitutional defects. (c–e) are monoatomic interstitial defects and (f) is the molecular H_2 interstitial inside the interlayer tetrahedral void (silver lines). Crystal structure images were rendered using the VESTA visualization program.[29]

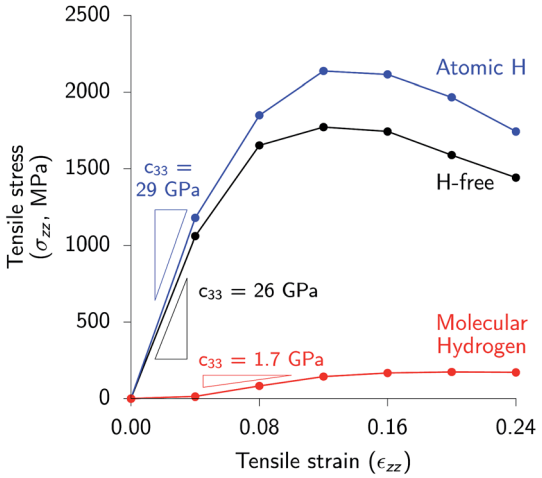

Fig. 2 The presence of molecular hydrogen interstitials reduces both the ultimate strength and elastic modulus by more than 90% compared to the hydrogen-free mackinawite.

defects are calculated in the 'iron-rich' chemical potential regime as defined in reference 19. This is appropriate for mackinawite under sour corrosion conditions, where mackinawite films are in thermodynamic equilibrium with iron.

The S-bonded monoatomic hydrogen interstitial and the interlayer H_2 interstitial have the lowest formation energies of all the defects considered and are therefore expected to dominate the hydrogen defect chemistry in mackinawite at low temperatures. Therefore, we will only consider the effect of these two defects on the mechanical properties in subsequent sections.

Finally, the formation energies of the stable monoatomic and molecular hydrogen interstitials in mackinawite are comparable to, but lower than, hydrogen defect formation energies in other similar layered material systems like MoS_2 ($\Delta G_f = 0.8$ eV and 1.4 eV for molecular and atomic interstitials, respectively[30]). This indicates a greater concentration of hydrogen defects at equilibrium in the mackinawite structure and also supports the choice of a high hydrogen concentration of H : Fe = 0.50 in the following simulations of mackinawite mechanical properties.

3.2. Mechanical response to uniaxial strain, ϵ_{zz}

The simulated uniaxial tensile test of the H-free mackinawite crystal yields a tensile strength of 1772 MPa and an elastic modulus of 26 GPa (Fig. 2), which is very similar to experimental and calculated values for out-of-plane elastic modulus for graphite,[31,32] indicating that the main forces operative in this simulation are van der Waals in the z-direction.

Repeating the simulation on a mackinawite crystal with S-bonded H interstitials, we find that both the ultimate strength and elastic modulus improve marginally to 2137 MPa and 29 GPa, respectively. This strengthening effect has been previously observed for other interstitial atoms K, Li and Cl in graphite.[21,31]

To understand the mechanism behind strengthening, we plot the charge redistribution due to hydrogen defect formation. Similar to the case of atomic interstitials like K and Cl in graphite as well as small organic molecular interstitials like tetracyanoethylene[33] in MoS_2, there is moderate charge transfer between the monoatomic interstitial and the mackinawite layers (Fig. 3a). This introduces new dipolar and hydrogen-bonding interactions between layers which complement the weak van der Waals interactions leading to strengthened interlayer bonds and better mechanical properties.

The mackinawite crystal weakens significantly in the presence of H_2 interstitials with both the yield stress and elastic modulus decreasing by over 90% to 173 MPa and 1.7 GPa, respectively. This is also similar to other molecular interstitials and intercalants in other layered systems like KCl and C_6H_6 in graphite.[13] In the absence of any charge transfer to the layered crystal (Fig. 3b), the closed-shell interstitial species introduces repulsive steric interactions between the host crystal sheets that undermine the attractive van der Waals interactions. This steric behavior of H_2 molecules has previously been observed on graphene monolayers, where the most stable physisorption site for H_2 molecules is the hollow of the hexagonal graphene ring, away from the electron densities of the C–C σ bonds.[34]

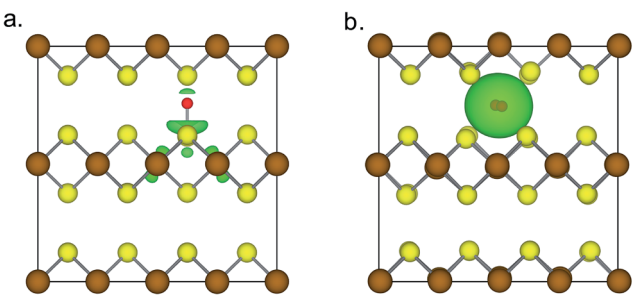

Fig. 3 Atomic H interstitials induce charge transfer to the mackinawite layers and create dipolar attractive interactions among layers leading to strengthening (a), whereas molecular H_2 interstitials induce only steric repulsion that weakens existing attractive van der Waals bonding (b).

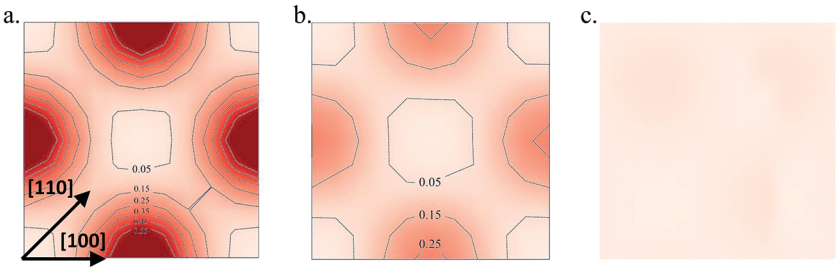

Fig. 4 Atomic H interstitials (a) strengthen inter-layer interactions leading to a sharper potential energy surface (PES) compared to that of hydrogen-free mackinawite (b). (c) Molecular H_2 interstitials weaken inter-layer attractive interactions leading to a very flat potential energy surface that enables easy inter-layer sliding and exfoliation. Each PES shown here spans 1 unit cell in the x- and y-directions and contour values are shown in eV per unit cell.

3.3. Mechanical response to shear strain, τ_{xz} and τ_{yz}

Sliding between layers is an inevitable and required mechanism during exfoliation of layered systems.[35] Therefore, resistance to interlayer sliding is an important part of overall resistance to mechanical damage. However, this resistance depends strongly on the specific direction of sliding. This dependence is described by potential energy surface (PES) maps that show the variation of potential energy of the layered system as one crystal sheet sliding over another one. The complete PES maps for hydrogen-free and hydrogen-containing mackinawite crystals in Fig. 4 show that [110] is the easy sliding direction with the lowest energy barriers while sliding along the [100] direction involves the largest activation barrier.

These PES descriptions can be directly related to the shear stress–strain behavior by observing that the resistance to sliding (*i.e.* the calculated shear stress for a given shear strain) is equal to the gradient of the change in potential energy in the given direction. To capture the impact of H-defects on the inter-layer binding, we plot stress–strain diagrams for shear strain along two representative directions, [100] and [110] that span the entire range of potential energy gradients.

In the easy-glide [110] direction, the hydrogen-free mackinawite crystal shows a maximum stress of 1279 MPa and a shear modulus of 11 GPa (Fig. 5), values that are similar to those observed for MoS_2.[26,36] Similar to the case of tensile strain, atomic H interstitials strengthen interlaminar bonding, making it difficult to shear the sheets relative to one another while H_2 interstitials degrade interlaminar bonding to such an extent that sliding becomes facile.

3.4. Hydrogen-induced exfoliation and impact on protectiveness of mackinawite passive films

The poor mechanical properties of mackinawite crystals containing H_2 interstitials suggest a plausible mechanistic explanation for easy spallation and concomitant poor protectiveness of mackinawite passive films. It is well known that epitaxially-grown passive films on metal surfaces undergo cracking and mechanical damage upon reaching a certain critical thickness in order to release epitaxial strain energy.[37] However, this mechanism is not operative in layered films like mackinawite, which are capable of accommodating all the epitaxial strain within the inter-layer van der Waals regions.[38] In this context, H-mediated exfoliation emerges as an important mechanism to explain the observed exfoliation and rupture of mackinawite films.

The effective degradation of interlayer bonds in mackinawite by hydrogen point defects suggest interlayer H_2 evolution as an effective exfoliation technique. In particular, in conducting films like mackinawite that admit easy intercalation of water and protons,[39] simple cathodic polarization can lead to proton discharge and hydrogen evolution internally, leading to

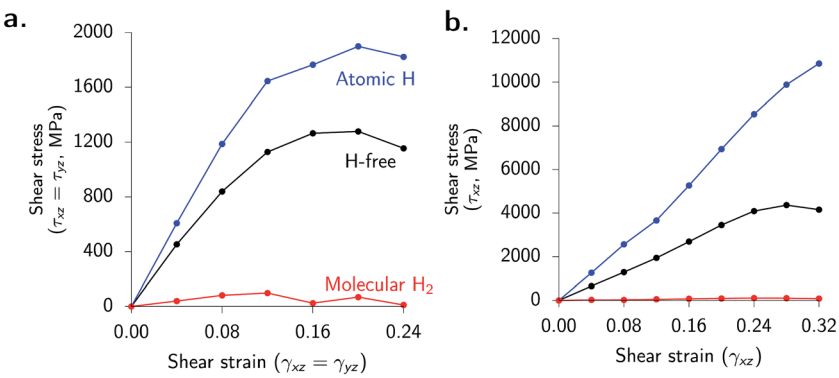

Fig. 5 Molecular H_2 interstitials weaken inter-layer binding and enable facile sliding along both the (a) [110] and (b) [100] directions. This reduced resistance to inter-layer sliding implies easier multi-layer exfoliation and consequently poorly protective mackinawite.

exfoliation. This is a process that can be exploited in other layered systems like 1T-MoS_2.

It must also be noted that both the high and low concentration of hydrogen defects lead to a similar weakening behavior in mackinawite. The significant weakening of interlaminar binding in the paper here was quantified in crystals containing a relatively high hydrogen concentration of H : Fe = 0.50 (qualitatively commensurate with the low hydrogen defect formation energies). A similar weakening is also found in crystals with lower hydrogen point defect concentration (H : Fe = 0.125, see Fig. S2 in the ESI†), indicating that these effects are experimentally accessible and relevant.

4. Summary

In order to understand the impact of hydrogen defects on the mechanical properties of layered systems, we performed *in silico* stress–strain tests on mackinawite crystals with monoatomic hydrogen interstitials and with interlayer molecular H_2 interstitials. Steric interactions due to molecular H_2 interstitials were found to severely degrade the attractive van der Waals interactions, enabling facile inter-layer sliding and exfoliation.

This finding provides a plausible explanation for the spontaneous cracking and spalling observed in these layered passive films. The difference in the mechanical behavior due to H and H_2 interstitials also suggests an effective non-destructive exfoliation technique involving electrochemical generation of H_2 molecules in the bulk of layered compounds like $Fe_{1+x}S$. Elucidation of this mechanism involves calculation of energy barriers involved in atomic H intercalation and subsequent H_2 evolution which will be the focus of our future work.

Acknowledgements

We gratefully acknowledge the support provided by BP PLC through the BP-MIT Center for Materials and Corrosion Research and by the National Science Foundation for the computational resources provided through the Texas Advanced Computing Center under Grant No. TG-DMR120025. This research used resources of the National Energy Research Scientific Computing Center, a DOE Office of Science User Facility supported by the Office of Science of the U.S. Department of Energy under Contract No. DE-AC02-05CH11231.

References

1 M. Lukowski, *et al.*, Enhanced Hydrogen Evolution Catalysis from Chemically Exfoliated Metallic MoS_2 Nanosheets, *J. Am. Chem. Soc.*, 2013, **135**(28), 10274–10277.
2 S. Patchkovskii, *et al.*, Graphene nanostructures as tunable storage media for molecular hydrogen, *Proc. Natl. Acad. Sci. U. S. A.*, 2005, **102**(30), 10439–10444.
3 M. Naguib, *et al.*, Two-Dimensional Nanocrystals Produced by Exfoliation of Ti_3AlC_2, *Adv. Mater.*, 2011, **23**(37), 4248–4253.
4 P. H. Tewari, M. G. Bailey and A. B. Campbell, Erosion-Corrosion of Carbon-Steel in Aqueous H_2S Solutions up to 120 °C and 1.6 MPa Pressure, *Corros. Sci.*, 1979, **19**(8), 573–585.
5 D. W. Shoesmith, *et al.*, Formation of ferrous monosulfide polymorphs during the corrosion of iron by aqueous hydrogen sulfide at 21 °C, *J. Electrochem. Soc.*, 1980, **127**(5), 1007–1015.
6 X. M. Dong, Q. C. Tian and Q. A. Zhang, Corrosion behaviour of oil well casing steel in H_2S saturated NACE solution, *Corros. Eng., Sci. Technol.*, 2010, **45**(2), 181–184.
7 D. Jiang and E. Carter, First principles assessment of ideal fracture energies of materials with mobile impurities: implications for hydrogen embrittlement of metals, *Acta Mater.*, 2004, **52**(16), 4801–4807.
8 J. Zahler, *et al.*, Role of hydrogen in hydrogen-induced layer exfoliation of germanium, *Phys. Rev. B: Condens. Matter Mater. Phys.*, 2007, **75**(3), 035309.
9 S. N. Rashkeev, *et al.*, Hydrogen-Induced Initiation of Corrosion in Aluminum, *J. Phys. Chem. C*, 2007, **111**(19), 7175–7178.
10 M. Youssef and B. Yildiz, Hydrogen defects in tetragonal ZrO_2 studied using density functional theory, *Phys. Chem. Chem. Phys.*, 2014, **16**(4), 1354–1365.
11 Z. Rak, *et al.*, Defect-induced rigidity enhancement in layered semiconductors, *Solid State Commun.*, 2010, **150**(27–28), 1200–1203.
12 O. C. Compton, *et al.*, Tuning the Mechanical Properties of Graphene Oxide Paper and Its Associated Polymer Nanocomposites by Controlling Cooperative Intersheet Hydrogen Bonding, *ACS Nano*, 2012, **6**(3), 2008–2019.
13 G. Yoon, *et al.*, Factors Affecting the Exfoliation of Graphite Intercalation Compounds for Graphene Synthesis, *Chem. Mater.*, 2015, **27**(6), 2067–2073.
14 W. Kohn and L. J. Sham, Self-Consistent Equations Including Exchange and Correlation Effects, *Phys. Rev.*, 1965, **140**(4A), A1133.
15 P. E. Blöchl, Projector augmented-wave method, *Phys. Rev. B: Condens. Matter Mater. Phys.*, 1994, **50**(24), 17953.
16 J. P. Perdew, K. Burke and M. Ernzerhof, Generalized Gradient Approximation Made Simple, *Phys. Rev. Lett.*, 1996, **77**(18), 3865.
17 G. Kresse and J. Furthmüller, Efficiency of ab-initio total energy calculations for metals and semiconductors using a plane-wave basis set, *Comput. Mater. Sci.*, 1996, **6**(1), 15–50.
18 G. Kresse and J. Furthmüller, Efficient iterative schemes for ab initio total-energy calculations using a plane-wave basis set, *Phys. Rev. B: Condens. Matter Mater. Phys.*, 1996, **54**(16), 11169.
19 A. Krishnamoorthy, *et al.*, Electronic states of intrinsic surface and bulk vacancies in FeS_2, *J. Phys.: Condens. Matter*, 2013, **25**(4), 045004.
20 H. J. Monkhorst and J. D. Pack, Special points for Brillouin-zone integrations, *Phys. Rev. B: Solid State*, 1976, **13**(12), 5188.
21 Y. Qi, *et al.*, Threefold Increase in the Young's Modulus of Graphite Negative Electrode during Lithium Intercalation, *J. Electrochem. Soc.*, 2010, **157**(5), A558–A566.

22 K. D. Kwon, *et al.*, Magnetic ordering in tetragonal FeS: evidence for strong itinerant spin fluctuations, *Phys. Rev. B: Condens. Matter Mater. Phys.*, 2011, **83**(6), 064402.
23 A. J. Devey, R. Grau-Crespo and N. H. de Leeuw, Combined density functional theory and interatomic potential study of the bulk and surface structures and properties of the iron sulfide mackinawite (FeS), *J. Phys. Chem. C*, 2008, **112**(29), 10960–10967.
24 M. Mullet, *et al.*, Surface chemistry and structural properties of mackinawite prepared by reaction of sulfide ions with metallic iron, *Geochim. Cosmochim. Acta*, 2002, **66**(5), 829–836.
25 S. Grimme, Semiempirical GGA-type density functional constructed with a long-range dispersion correction, *J. Comput. Chem.*, 2006, **27**(15), 1787–1799.
26 H. Peelaers and C. Van de Walle, Elastic Constants and Pressure-Induced Effects in MoS_2, *J. Phys. Chem. C*, 2014, **118**(22), 12073–12076.
27 J. Klimes, D. Bowler and A. Michaelides, van der Waals density functionals applied to solids, *Phys. Rev. B: Condens. Matter Mater. Phys.*, 2011, **83**(19), 195131.
28 S. Denholme, *et al.*, Pressure-dependent magnetization and magnetoresistivity studies on tetragonal FeS (mackinawite): revealing its intrinsic metallic character, *Sci. Technol. Adv. Mater.*, 2014, **15**(5), 055007.
29 K. Momma and F. Izumi, VESTA: a three-dimensional visualization system for electronic and structural analysis, *J. Appl. Crystallogr.*, 2008, **41**(3), 653–658.
30 Z. Zhu, H. Peelaers and C. Van de Walle, Hydrogen intercalation in MoS_2, *Phys. Rev. B*, 2016, **94**(8), 085426.
31 E. Ziambaras, *et al.*, Potassium intercalation in graphite: a van der Waals density-functional study, *Phys. Rev. B: Condens. Matter Mater. Phys.*, 2007, **76**(15), 155425.
32 T. Bjorkman, *et al.*, van der Waals Bonding in Layered Compounds from Advanced Density-Functional First-Principles Calculations, *Phys. Rev. Lett.*, 2012, **108**(23), 235502.
33 Y. Jing, *et al.*, Tuning electronic and optical properties of MoS_2 monolayer *via* molecular charge transfer, *J. Mater. Chem. A*, 2014, **2**(40), 16892–16897.
34 J. Arellano, *et al.*, Density functional study of adsorption of molecular hydrogen on graphene layers, *J. Chem. Phys.*, 2000, **112**(18), 8114–8119.
35 D. Tang, *et al.*, Nanomechanical cleavage of molybdenum disulphide atomic layers, *Nat. Commun.*, 2014, **5**, 3631.
36 T. Liang, *et al.*, First-principles determination of static potential energy surfaces for atomic friction in MoS_2 and MoO_3, *Phys. Rev. B: Condens. Matter Mater. Phys.*, 2008, **77**(10), 104105.
37 G. C. Wood and J. Stringer, The adhesion of growing oxide scales to the substrate, *J. Phys. IV*, 1993, **3**(C9), 65–74.
38 Y. Shi, H. Li and L. Li, Recent advances in controlled synthesis of two-dimensional transition metal dichalcogenides *via* vapour deposition techniques, *Chem. Soc. Rev.*, 2015, **44**(9), 2744–2756.
39 D. Munoz-Santiburcio, C. Wittekindt and D. Marx, Nanoconfinement effects on hydrated excess protons in layered materials, *Nat. Commun.*, 2013, **4**, 2349.

